Aza- and Mixed Thia/Aza-Macrocyclic Receptors with Quinoline-Bearing Pendant Arms for Optical Discrimination of Zinc(II) or

Quinoline-Functionalized Pendant Arm Derivatives of Aza- and Mixed Thia/Aza-Macrocyclic Receptors for Zn^{2+}/Cd^{2+} Optical Discrimination

Alessandra Garau,*[a] M. Carla Aragoni, [a] Massimiliano Arca,[a] Andrea Bencini,[b] Alexander J. Blake,[c] Claudia Caltagirone,[a] Claudia Giorgi,[b] Vito Lippolis,*[a] Mariano Andrea Scorciapino[a]

[a] Dr. A. Garau, Prof. M. C. Aragoni, Prof. M. Arca, Prof. C. Caltagirone, Prof. V. Lippolis, Dr. M.A. Scorciapino
Dipartimento di Scienze Chimiche e Geologiche
Università degli Studi di Cagliari
S.S. 554 Bivio per Sestu, I-09042 Monserrato (CA), Italy
E-mail: agarau@unica.it, lippolis@unica.it
[b] Prof. A. Bencinii, Prof. C. Giorgi
Dipartimento di Chimica "Ugo Schiff"
Università degli Studi di Firenze
Via della Lastruccia 3, I-50019 Sesto Fiorentino, Firenze, Italy
[c] Prof. A. J. Blake, School of Chemistry, University of Nottingham, University Park NG7 2RD Nottingham, UK

Abstract. Herein we describe the synthesis and coordination properties of two new fluorescent chemosensors, **L1** and **L2**, featuring [9]aneN$_3$ (1,4,7-triazacyclononane) and [12]aneNS$_3$ (1-aza-4,7,10-trithiacyclododecane) as receptor units, respectively, and a quinoline pendant arm with an amide group as a functional group spacer. The optical responses of **L1** and **L2** in the presence of several metal ions were analysed in MeCN/H_2O (1:4 v/v) solutions. A selective Chelation Enhancement of Fluorescence (CHEF) effect was observed in the presence of Zn^{2+} in the case of **L1**, and in the presence of Cd^{2+} in the case of **L2,** following the formation of a 1:1 and a 1:2 metal-to-ligand complex, respectively, as also confirmed by potentiometric measurements. ^{1}H-NMR measurements in $CD_3CN/CDCl_3$ (7:3 v/v) in combination with molecular mechanics calculations allowed a deeper insight into the nature of the complex species that **L1** and **L2** can form with Zn^{2+} and Cd^{2+}, respectively.

Introduction

In the last decades, fluorescent chemosensors have acquired an important role in the recognition and sensing of metal cations, inorganic/organic anions and small neutral molecules with applicative implications in chemical, biological and environmental sciences.[1-6]

The excellent application perspectives of fluorescent chemosensors are due to their obvious merits of unmatched ease of use, high sensitivity and low cost.[7]

In particular, a very active area of research is related to their use in the development of optical methodologies for the selective detection and quantification of metal ions such as Zn^{2+} [4a,8-12] and Cd^{2+},[4a,12-20] due to the intrinsic difficulty encountered in discriminating these two metal ions, which can be attributed to their common closed-shell d^{10} configuration and highly similar chemical properties.

Zinc is the second most abundant and essential transition element in living cells after iron. This metal plays highly crucial roles in many biological processes such as regulation of apoptosis, signal transmission, gene expression and enzyme function.[21,22] It represents the structural cofactor of many Zn^{2+}-containing enzymes and DNA-binding proteins. The imbalance of Zn^{2+}, whether as an excess or deficit, is linked to severe neurological disorders and growth defects. Zinc deficiency can lead to various diseases such as hair loss, retarded growth in children, brain disorders and various neurological dysfunctions such as Alzheimer's disease, epilepsy and ischemic stroke.[23,24] However, it becomes cytotoxic if present in significant excess and unbalanced metabolism may lead to skin disease, diabetes, prostatic adenocarcinoma and pancreatic islets dysfunction.[25]

On the other hand, Cd^{2+}, in common with other heavy metal ions, is still used in many industrial processes and the resulting high level of contamination in soil, water and food is raising a great concern.[26] Living organisms readily absorb Cd^{2+} from the environment, resulting in dangerous levels of cellular concentration and adverse effects upon human health.[27-30] Excessive exposure of cadmium(II) is reported to have toxic effects on procreation, bones, kidney, and nerve systems, resulting in renal dysfunction, metabolism disorders, and pulmonary, prostatic and renal cancer.[31-34]

Consequently, the design of novel molecular sensors that can selectively recognise zinc(II) and cadmium(II) among other metal ions is a challenging task of primary importance.

The most common approach to the synthesis of selective fluorescent chemosensors is to covalently link a fluorogenic fragment (signaling unit) to a guest-binding site (receptor unit) *via* an appropriate spacer. An optical signal, such as an enhancement or quenching of the fluorescence emission of the signaling unit, accompanies the host-guest interaction of the target species with the receptor unit and is used to quantify the detection process, in terms of binding constant, stoichiometry of the resultant complex, selectivity and sensitivity.

The choice of the signaling and the receptor units can be critical to achieve the thermodynamic and/or optical selectivity of the fluorescent probe, particularly if a direct interaction between the fluorophore and the target species is possible.[35a]

To easily achieve fluorescent chemosensors showing at least the optical selectivity for a given metal ions (this is still a

favourable case for analytical applications as compared to that of chemosensors having both thermodynamic and optical selectivity), in the last decade, we have adopted the synthetic strategy of linking to a predefined receptor unit (not necessarily having a binding selectivity for the substrate considered), different fluorogenic fragments counting on a "synergic cooperation" between the two units of the resulting conjugated chemosensors in determining at least the optical selectivity (the "synergic cooperation" can be recognized in the manifold of electronic levels associated with a given combination of receptor and signaling units, which can be selectively perturbed by a metal centre despite the absence of a binding affinity). [35-44]

Among others, great attention has been focused on the macrocycles 1,4,7-triazacyclononane ([9]aneN$_3$) and 1-aza-4,7,10-trithiacyclododecane ([12]aneNS$_3$) as receptor units. The binding properties of these ligands can be easily tuned through functionalization of the secondary amines with pendant arms bearing different coordinating groups to generate ligands with an increased number of donor atoms and different supramolecular functionalities.[45] In fact, several kind of fluorogenic fragments, in particular quinoline-based ones, have been covalently linked to [9]aneN$_3$ and [12]aneNS$_3$, as reported in Scheme 1, and despite the fact that all macrocycles can form stable 1:1 complexes with a variety of heavy metal ions, different optical selectivities have been recorded for the resulting chemosensors depending on the experimental conditions used.[38, 41, 43, 44]

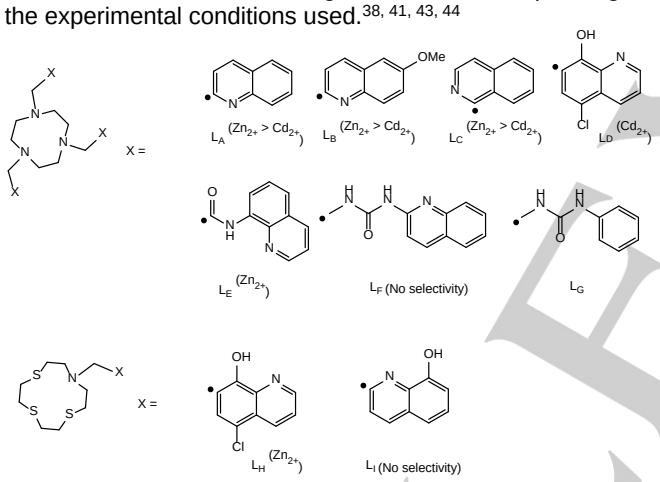

Scheme 1. Chemical structures of [9]aneN$_3$- and [12]aneNS$_3$-based fluorescent chemosensors reported in the literature with the observed optical selectivity in brackets. Dots indicate the linkage point of the pendant arm(s).

In particular, while [9]aneN$_3$-based chemosensors **L$_A$**, **L$_B$**, and **L$_C$** showed a marked Chelation Enhancement of Fluorescence (CHEF) effect in the presence of Zn^{2+} together with a reduced response in the presence of Cd^{2+};[43] ligands **L$_D$** and **L$_E$** showed a different behaviour: the former is optically selective only for Cd^{2+},[44b] the latter only for Zn^{2+},[44a]. A selective CHEF effect for Zn^{2+} was observed for the [12]aneNS$_3$-based ligand **L$_H$**.[41]

Following our interest in both the coordination chemistry of [9]aneN$_3$ and [12]aneNS$_3$ derivatives and their use in the development of chemosensors and supramolecular systems,[35-42,44] herein we describe the synthesis and recognition/sensing properties towards heavy metal ions of two new quinoline-containing derivatives of these macrocycles characterized by the presence of a functional amide-group as spacer between the receptor and the signaling units (Figure 1).

The main goal was to study the effects on the binding/sensing properties towards metal ions of the designed ligands, which show different binding domains determined by the different macrocyclic units, and to achieve Zn^{2+}/Cd^{2+} optical discrimination with structurally similar fluorescent chemosensors (Figure 1).

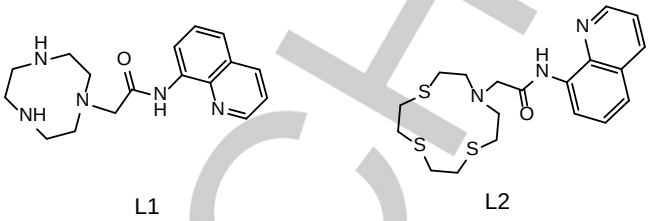

Figure 1. Chemical structures of the ligands discussed in this paper**.**

Results and Discussion

Synthesis of L1 and L2. L1 was prepared by reacting 1,4,7-triazacyclononane-1,4-dicarboxylic acid di-*tert*-butyl ester with 1 equiv. of 2-chloro-*N*-8-quinolinylacetamide in acetonitrile in the presence of K_2CO_3, followed by deprotection of the amine group with trifluoroacetic acid.

L2 was prepared by reacting 1-aza-4,7,10-trithiacyclododecane with 1 equiv. of 2-chloro-*N*-8-quinolinylacetamide in acetonitrile and in the presence of K_2CO_3 (for synthetic details see Supporting Information, SI).

Metal complexation by L1 and L2: spectrophotometric measurements. In order to analyse the potentialities of the new ligands as fluorescent chemosensors for metal ions recognition, we performed a spectrophotometric and spectrofluorimetric screening of the sensing ability of **L1** and **L2** toward several metal ions, in particular Cd^{2+}, Co^{2+}, Cu^{2+}, Fe^{3+}, Hg^{2+}, K^+, Mg^{2+}, Mn^{2+}, Ni^{2+}, Zn^{2+} and Pb^{2+} (as nitrate or perchlorate salts).

The absorption spectrum of solutions of **L1** and **L2** in MeCN/H_2O (1:4 v/v) shows a sharp band at 239 nm (ε = 23950 for **L1** and 26000 M^{-1} cm^{-1} for **L2**, respectively) and a broad one at 307 nm (4190 for **L1** and 5320 M^{-1} cm^{-1} for **L2**, respectively). The former is related to the weak emission band at 505 nm with a low fluorescence quantum yield (Φ = 0.015 and 0.016 for **L1** and **L2**, respectively).

Significant changes in the UV-vis spectrum of **L1** were observed only upon addition of increasing amounts of Zn^{2+}, Cu^{2+} and Hg^{2+} to a MeCN/H_2O (1:4 v/v) solution of the ligand at pH = 7.4 (MOPS buffer) [MOPS = 3-*N*-morpholino-propansulfonic acid] (see Figure S1, SI), and in the presence of Cd^{2+}, Cu^{2+} and Hg^{2+} ions in the case of **L2** under the same experimental conditions used for **L1** (Figure S2, SI). Particularly, the intensity of the bands at 239 and 307 nm decreased, whereas two new bands appeared at about 260 and 360 nm.

Considering the fluorescence emission, in the case of **L1**, a significant CHEF effect was observed only upon addition of Zn^{2+} at pH = 7.4 (Figure 1a), while **L2** similarly changed its emission OFF state in the presence of Cd^{2+} with a lower CHEF effect also in the presence of Zn^{2+} (Figure 1b). The other metal ions considered did not affect the emission OFF state of **L1** and **L2** (Figure 1) under the experimental conditions considered.

The optical selectivity for Zn^{2+} and Cd^{2+} displayed by **L1** and **L2**, respectively, prompted us to further investigate their binding properties towards these metal ions. A spectrophotometric titration of **L1** with Zn^{2+} in MeCN/H_2O (1:4 v/v) at pH = 7.4, showed the presence of three isosbestic points at 250, 285 and 345 nm (Figure 2a), while a spectrofluorimetric titration under the same experimental conditions, confirmed the significant selective CHEF effect at 505 nm (Figure 2c).

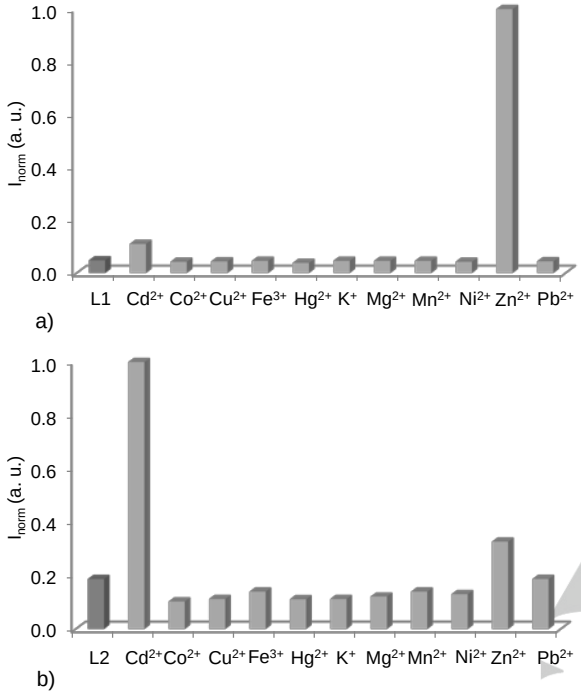

Figure 1. a) Normalized fluorescence emission of a) **L1** and b) **L2** upon addition at pH = 7.4 (MOPS buffer) of 1 equiv. of Cd^{2+}, Co^{2+}, Cu^{2+}, Fe^{3+}, Hg^{2+}, K^+, Mg^{2+}, Mn^{2+}, Ni^{2+}, Zn^{2+} and Pb^{2+} (MeCN/H_2O 1:4 v/v, 298 K, λ_{exc} = 330 nm, λ_{em} = 505 nm.

The fluorescence emission intensity reached the maximum after the addition of about 1.0 equiv. of Zn^{2+}, with a quantum yield of 0.077. The inflection points in both the absorbance and fluorescence intensity/molar ratio plots (Figs. 2b and 2d) would suggest the presence in solution of a 1:1 metal-to-ligand complex.

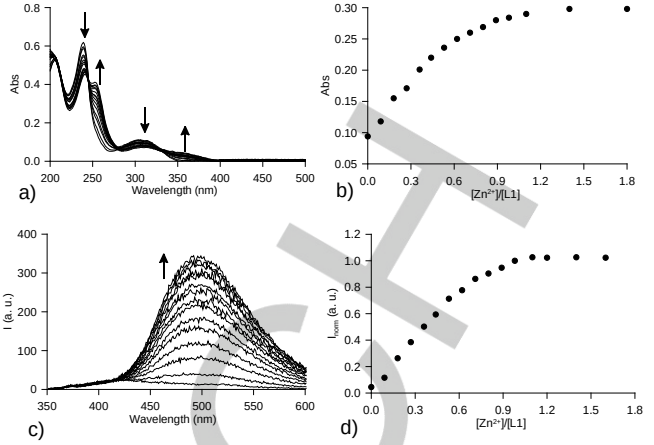

Figure 2. a) and b) Changes in the Uv-Vis spectrum and absorbance at 260 nm *versus* molar ratio plot for **L1**, respectively, upon addition of increasing amounts of Zn^{2+}; c) and d) changes in the emission spectrum and normalized fluorescent intensity *versus* molar ratio plot for **L1**, respectively, upon addition of increasing amounts of Zn^{2+} ([**L1**]= $2.58 \cdot 10^{-5}$ M, MeCN/H_2O (1:4 v/v), pH = 7.4 (MOPS buffer), 298 K, λ_{exc} = 330 nm, λ_{em} = 505 nm).

The spectrophotometric titration of **L2** with Cd^{2+} at pH = 7.4 in MeCN/H_2O (1:4 v/v) showed the presence of three isosbestic points at 250, 286 and 340 nm (Figure 3a), while a spectrofluorimetric titration under the same experimental conditions confirmed the significant selective CHEF effect at 505 nm (Figure 3c).

The absorption and fluorescence emission intensity linearly increase up to the addition of about 0.4 equivs. of the metal ion with a quantum yield of 0.068. These observations strongly suggest the formation in solution of a complex with a 1:2 metal-to-ligand stoichiometry.

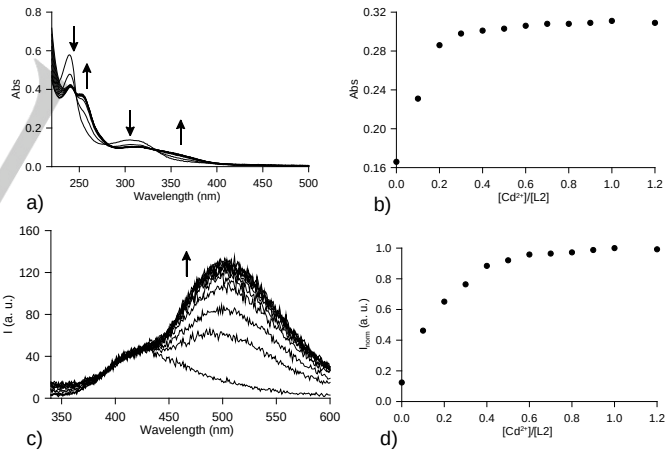

Figure 3. a) and b) Changes in the Uv-Vis spectrum and absorbance at 260 nm *versus* molar ratio plot for **L2**, respectively, upon addition of increasing amounts of Cd^{2+}; c) and d) changes in the emission spectrum and normalized fluorescent intensity *versus* molar ratio plot for **L2**, respectively, upon addition of increasing amounts of Cd^{2+} ([**L2**]= $2.24 \cdot 10^{-5}$ M, MeCN/H_2O (1:4 v/v), pH = 7.4 (MOPS buffer), 298 K, λ_{exc} = 330 nm, λ_{em} = 505 nm).

In order to study ion competition, two types of measurements were performed in MeCN/H_2O (1:4 v/v) at pH = 7.4 on both ligands: a) 5 equivs. of M^{n+} were added to an equimolar solution of **L1** and Zn^{2+} or **L2** and Cd^{2+} (Figure 4); b) 1 equiv. of Zn^{2+} (Cd^{2+}) was added to an equimolar solution of **L1** (**L2**) and M^{n+} (M^{n+} = Cd^{2+} in the case of **L1** or Zn^{2+} in the case of **L2**, along with Co^{2+}, Cu^{2+}, Fe^{3+}, Hg^{2+}, K^+, Mg^{2+}, Mn^{2+}, Ni^{2+} and Pb^{2+} for both ligands (Figure S3). Similar results were obtained in both cases. The analysis of the Figures 4 and S3, shows that Cu^{2+} and Hg^{2+} in the case of **L1**, and only Cu^{2+} in

the case of **L2** can compete in ligand binding with Zn^{2+} and Cd^{2+} ions**,** respectively, inducing a significant decrease of the fluorescence emission.
In the case of **L1**, the competition of Cu^{2+} is well supported by the high affinity of this metal ion for the ligand, as confirmed by potentiometric measurements (see below).
A similar behavior was also found in the case of $\mathbf{L_E}$, which contains three pendant arms as in **L1** (Scheme 1). Cu^{2+} and Hg^{2+} were found to compete with Zn^{2+} in the binding process causing a remarkable quenching of the fluorescence emission of the preformed 1:1 $Zn^{2+}/\mathbf{L_E}$ metal complex. No competition by Cu^{2+} and Hg^{2+} was observed in the case of ligands $\mathbf{L_A}$-$\mathbf{L_D}$ and $\mathbf{L_H}$ (Scheme 1).

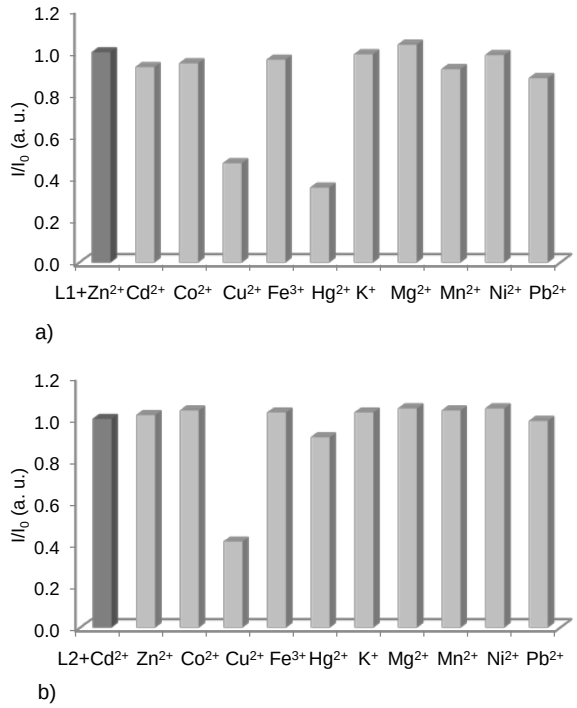

Figure 4. Normalized relative fluorescence emission intensity for the ion competition study performed by adding five equivs. of M^{n+} to an equimolar solution of **L1** and Zn^{2+} a) and to an equimolar solution of **L2** and Cd^{2+} b) ([**L1**] = $2.58 \cdot 10^{-5}$ M, [**L2**] = $2.24 \cdot 10^{-5}$ M, MeCN/H_2O (1:4 v/v), pH 7.4 (MOPS buffer), 298 K, λ_{exc} = 330 nm, λ_{em} = 505 nm.

Metal complexation by L1 and L2: potentiometric measurements. In order to further analyse the binding features of **L1** and **L2** in solution, and to gain an insight into the thermodynamic selectivity of the two ligands, we studied metal complexation by means of potentiometric measurements in MeCN/H_2O (1:4 v/v) solutions a 298 K. This solvent mixture ensures sufficient solubility (at least 5 x 10^{-4} M) of both ligands and most of their metal complexes over a wide pH range (2-10.5). However, in the case of Pb^{2+} and Hg^{2+} complexation with **L1**, and Hg^{2+} complexation with **L2**, precipitation occurs above pH 7.5, probably due to the formation of insoluble hydroxo complexes that prevents the speciation study in the alkaline pH region.
As a necessary prerequisite for the study of metal complexation, we initially analyzed the acid-base properties of **L1** and **L2**, determining their protonation constants that are reported in Table 1. Figure S4 (see SI) displays the distribution diagrams of the protonated species at different pH values.

Table 1. Protonation constants (log *K*) of **L1** and **L2** [*I* = 0.10 M, 298 K, MeCN/H_2O (1:4 v/v)].

Reaction	L1	L2
$L + H^+ = (HL)^+$	10.20(3)	7.96(2)
$(HL)^+ + H^+ = (H_2L)^{2+}$	6.02(9)	3.37(1)
$(H_2L)^{2+} + H^+ = (H_3L)^{3+}$	3.21(9)	=

The values reported in Table 1 reflect the structural characteristics of the ligands that contain two remarkably different macrocyclic moieties in terms of number of protonatable amine groups. **L1** can form up to three-protonated species and displays a remarkably high first protonation constant (log *K* = 10.20), slightly lower than that reported for non-functionalised [9]aneN_3 in water solution (log *K* = 10.60).[45] Similarly, the second protonation constant (log *K* = 6.02) is somewhat lower than that found for [9]aneN_3 in water (log *K* = 6.80),[45] but it is higher, however, than the protonation constant of quinoline (log *K* = 4.94).[46] These observations strongly suggest that the second protonation equilibrium of **L1** still occurs on an amine group of the macrocyclic unit. Considering that [9]aneN_3 has a very poor tendency to form a three-protonated species in water,[47] the third protonation step of **L1** is likely to occur on the heteroaromatic nitrogen of the quinoline moiety.
L2 exhibits only two protonation steps. Aliphatic amine groups are normally more basic that the quinoline nitrogen and the first protonation constant (log *K* = 7.96) of **L2** is similar to that previously found for other ligands containing the [12]aneNS_3 unit.[41] This would suggest the first protonation step occurs on the tertiary nitrogen atom of the NS_3 macrocyclic unit, while quinoline would only be involved in proton binding in the second protonation equilibrium.
As a first analysis of the metal binding ability of **L1** and **L2**, we performed potentiometric titrations in the presence of five selected metal ions, namely Cu^{2+}, Zn^{2+}, Cd^{2+}, Pb^{2+} and Hg^{2+}. The species formed in solution and the corresponding formation constant are reported in Table 2, while the distribution diagrams of the complexes are displayed in Figures 5 (Zn^{2+} complexes of **L1**) and Figure 6 (Cd^{2+} complexes of **L2**) and Figures S5-S7 (see SI).

Table 2. Formation constants (log *K*) of **L1** and **L2** with Cu^{2+}, Zn^{2+}, Cd^{2+}, Pb^{2+} and Hg^{2+} [*I* = 0.10 M, 298 K, MecN/H_2O (1:4 v/v)].

Reaction	Cu^{2+}	Zn^{2+}	Cd^{2+}	Pb^{2+}	Hg^{2+}
L1 + M^{2+} = $[ML1]^{2+}$	15.6(7)	11.79(4)	8.6(1)	10.1(1)	11.2(2)
$[ML1]^{2+}$ + OH^- = $[ML1(OH)]^+$	6.52(9)	6.70(9)	5.1(1)		
$[ML1(OH)]^+$ + OH^- = $[ML1(OH)_2]$	5.32(1)	5.61(9)			
L2 + M^{2+} = $[ML2]^{2+}$	9.21(4)	8.89(3)	8.1(3)	9.28(9)	9.8(4)
$[ML2]^{2+}$ + $2OH^-$ = $[ML2(OH_2)]$	11.5(4)	12.03(3)	10.6(7)	13.04 (8)	
2**L2** + M^{2+} = $[M(L2)_2]^{2+}$	18.1(1)	17.9(1)	16.5(1)	18.3(1)	18.9(1)
L2 + $[ML2]^{2+}$ = $[M(L2)_2]^{2+}$	8.9	9.0	8.0	9.1	9.1

L1 forms stable complexes with 1:1 metal-to-ligand stoichiometry with all five metal ions considered. Beside the formation of the complexes $[ML1]^{2+}$, facile deprotonation of metal-bound water molecules is observed to give mono- and dihydroxylated complexed species, which are the most abundant above *ca.* pH 7 in the case of Cu^{2+} and Zn^{2+} (Table 2 and Figures 5 and S5). A stable monohydroxo-complex $[CdL1(OH)]^+$ is formed also in case of the Cd^{2+} complexation, while precipitation at alkaline pH values precludes the analysis of the species formed by the Pb^{2+} and Hg^{2+} complexes above pH 7. Interestingly enough, the stability constant values found for the formation of $[ML1]^{2+}$ complexes are rather similar to those reported for the corresponding complexes with the simple macrocycle [9]aneN$_3$ in water solution[35b] and increase in the order $Cd^{2+}<Pb^{2+}<Zn^{2+}<Cu^{2+}$, following the same trend observed for [9]aneN$_3$. These results suggest that the metals are coordinated by the polyamine macrocycle unit, while the amide side arms are weakly involved or not involved in metal binding, at least in aqueous media. As already suggested for [9]aneN$_3$,[45b] the lower stability of larger metal ions, such as Cd^{2+}, might reflect the small and rigid cavity of the macrocycle. The strong tendency to form hydroxo-species, displayed in particular by the $[CuL1]^{2+}$ and $[ZnL1]^{2+}$ complexes, is generally attributed to metal centres not coordinatively saturated by the ligand donors. This corroborates the hypothesis the amide group does not participate in metal coordination, at least in the case of the smaller and more acidic Cu^{2+} and Zn^{2+} ions. Unfortunately, no comparison can be made between Hg^{2+} complexation by **L1** and [9]aneN$_3$. In fact, the stability constant of the **L1** complex with Hg^{2+} has been calculated without considering possible chloride complexation (see SI) and it is to be considered a conditional constant.

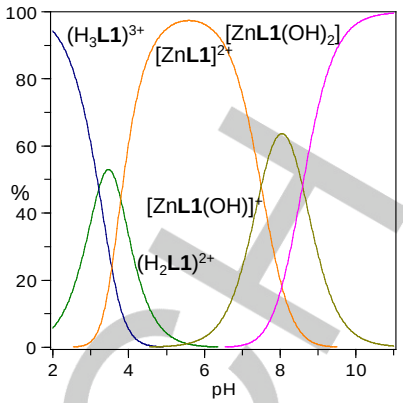

Figure 5. Distribution diagram of the complex species formed by **L1** and Zn^{2+} in 1:1 molar ratio [298 K, NaCl 0.10 M in MeCN/H_2O (1:4 v/v)].

Differently from **L1**, **L2** forms not only 1:1 metal complexes, but also species with a 1:2 metal-to-ligand stoichiometry (Table 2, Figures S6 and S7 in SI). With regard to the 1:1 complexes, the data in Table 2 show that all the $[ML2]^{2+}$ complexes (M = Cu^{2+}, Zn^{2+}, Cd^{2+}, Pb^{2+} and Hg^{2+}) are less stable than the corresponding $[ML1]^{2+}$ ones, in agreement with the lower σ-donor ability of thiol groups of the NS_3 donor set of **L2** with respect to the aliphatic amine donors of the [9]aneN$_3$ unit of **L1**. The decrease in stability is actually more evident in the case of the 1:1 Cu^{2+} and Zn^{2+} complexes, in agreement with the more marked 'hard' character of these metal ions, which can strongly reduce their affinity for 'soft' donors, such as the sulphur atoms of **L2**.

The decrease in stability is reduced in the case of the softer Cd^{2+}, Pb^{2+} and Hg^{2+} ions (the stability constants of their $[ML2]^{2+}$ complexes are only *ca.* 0.5, 0.8 and 1.4 log units lower that those found for the corresponding $[ML1]^{2+}$ species). As a result, the $[ML2]^{2+}$ complexes with the five metal ions under investigation, display rather similar stability constants, ranging between 9.8 and 8.1 log units (Table 2).

Similarly to **L1**, the $[ML2]^{2+}$ complex affords hydroxylated species at alkaline pH values (Figure 6). In this case, however, the constant for the addition of a single hydroxide anion to the metal cannot be calculated and only the overall constants for the equilibrium $[ML2]^{2+}$ + $2OH^-$ = $[ML2(OH)_2]$ can be determined. This is normally due to the formation of mono- and di-hydroxo species at very similar pH values, which prevents to potentiometrically distinguish the equilibria relative to the separate addition of a single hydroxide anion to the $[ML]^{2+}$ and $[ML(OH)]^+$ species and to calculate the corresponding addition constants. However, the formation of hydroxylated species is indicative of metal coordination spheres not saturated by the ligand donors, which favour deprotonation of metal-bound water molecules. Furthermore, the formation of $[M(L2)_2]^{2+}$ species in solution represents the most striking difference from **L1**. In fact, the $[ML2]^{2+}$ complexes can add a second ligand molecule to form complexes having a 1:2 metal-to-ligand stoichiometry, the constants for the addition of a second **L2** molecule to the $[ML2]^{2+}$ complexes being similar or slightly lower than the formation constants of the 1:1 species. This may reflect the presence in the 1:1 $[ML2]^{2+}$ complexes of free binding sites, which can be used to interact with water molecules or with a second ligand molecule. The high tendency of **L2** to give $[M(L2)_2]^{2+}$ complexes strongly influence the solution chemistry of this ligand in the presence of the five selected metal ions. In fact, 1:2 complexes are the most abundant species even in the presence of 1 equiv. of **L2** in a wide pH range (Figure 6) and become almost the unique species in

the presence of 2 equivs. of ligand. The 1:1 di-hydroxo complexes ([M**L2**$(OH)_2$] species) are formed in relevant percentages only at alkaline pH values (generally above pH 9) in the presence of 1 equiv. of ligand and are almost absent from solution containing 2 equivs. of **L2** even at strongly alkaline pH values (Figure 6).

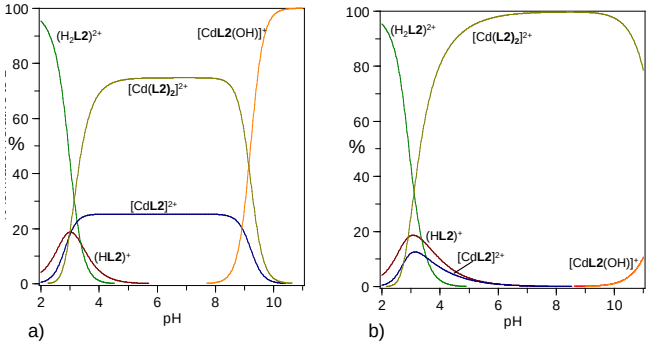

Figure 6. Distribution diagrams of the complex species formed by **L2** in the presence of a) 1 equiv. and b) 0.5 equivs. of Cd^{2+} [298 K, NaCl 0.10 M in MeCN/H_2O (1:4 v/v)].

Metal complexation by L1 and L2: ^{1}H-NMR measurements. In order to gain a deeper insight into the possible nature of the Cd^{2+} complex with **L2** and the Zn^{2+} complex with **L1**, we also analyzed the complexation of these metal ions by means of ^{1}H-NMR measurements. The MeCN/H_2O (1:4 v/v) solvent mixture used in UV-Vis, fluorescence emission and potentiometric measurements could not be used at the higher metal and ligand concentrations required for ^{1}H-NMR measurements (concentration *ca.* $1.0 \cdot 10^{-2}$ M) and, therefore, the spectra were recorded in $CD_3CN/CDCl_3$ (7:3 v/v).

Figure 7 shows changes observed in the ^{1}H-NMR spectrum upon titration of **L2** with Cd^{2+} ion. ^{1}H resonance assignments are indicated with numbers corresponding to those reported in Figure 7 for the related H atom(s). Signal assignment was based on relative area, fine structure analysis and comparison with chemical shift predictions.[48–50]

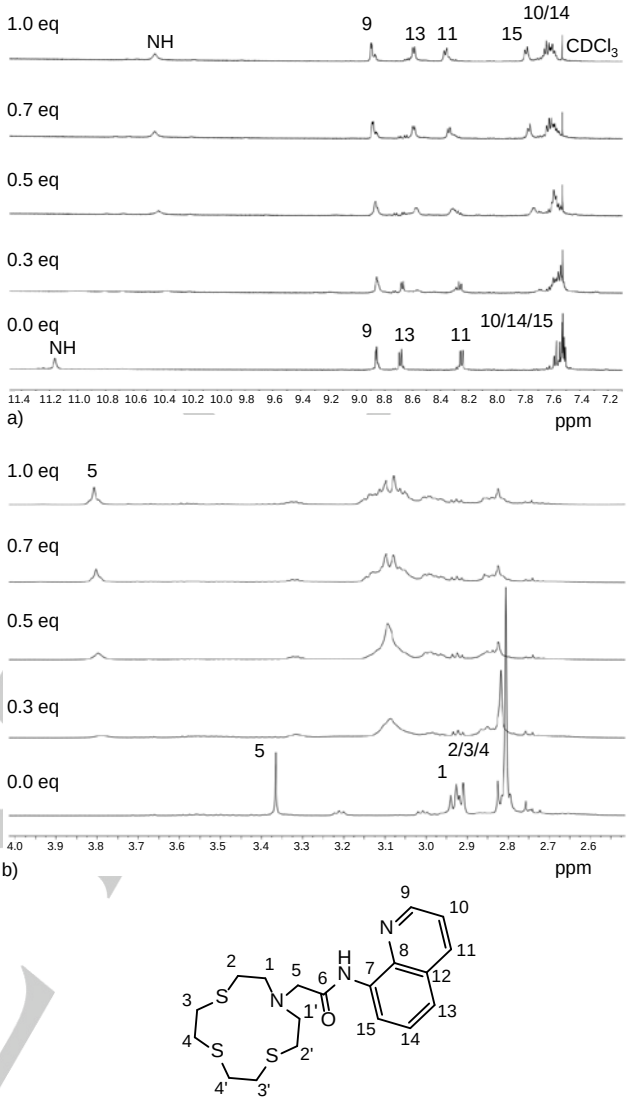

Figure 7. a) High and b) low field region of the ^{1}H-NMR spectra of **L2** in the presence of increasing amounts of Cd^{2+}.

It is evident how resonances assigned to the macrocycle ethylene groups, between 2.8 and 3.0 ppm, dramatically changed upon addition of Cd^{2+} ions. Both the shift and the change in the fine structure are a clear indication of the macrocycle being directly involved in the coordination of the metal ion. In particular, the most noticeable change can be observed for the sharp singlet resonance at 2.82 ppm, attributed to the protons H3 and H4. In the free ligand, the macrocycle ethylene groups farther from the pendant arm, are mobile and free to change configuration. These rapid interconversions are reflected by the sharp singlet. Upon coordination of the Cd^{2+} ion, the macrocyclic unit in **L2** becomes more rigid and overall configuration fixed. The protons of the ethylene groups, H3 and H4 turn from 1st to 2nd order spin system and this is reflected by the appearance of more complex multiplets in the ^{1}H-NMR spectrum.

However, the largest shift is observed for the amide proton and the methylene protons adjacent to the carbonyl group (H5 in Figure 7). This cannot be explained by the exclusive coordination of the metal ions by the macrocyclic unit and let us hypothesize the direct involvement of the carbonyl itself as confirmed by the fine structure of the resonance assigned

to proton H5. Upon addition of Cd^{2+} ions, a progressive change is observed from one singlet to two doublets with a remarkable roof effect. This is a clear indication of reduced mobility, so that the two geminal protons become magnetically inequivalent and their mutual J-coupling can be observed. In addition, both the proton H5 and the NH signals show the formation of only one complex in equilibrium with the free ligand, whose relative concentration progressively increases along the titration. Exchange rate appears to be sufficiently slow on the NMR timescale, so that two distinct resonances can be observed at the position of the free ligand and the complex, respectively. Presumably as already observed in solution for ligand $\mathbf{L_E}$ (Scheme 1),[44] also in **L2** there could be the possibility of an intramolecular H-bond between the amide NH donor from the pendant arm, and either the carbonyl from the amide group or the quinoline nitrogen acceptor on the same pendant arm. Thus, the NH shift to lower frequency observed upon metal coordination might be due either to the breaking of this H bond upon complex formation or to the electronic rearrangement of the amide group as a consequence of a possible carbonyl involvement in metal coordination.

From the analysis of the aromatic portion of the ^{1}H-NMR spectra, two resonances for each of the aromatic protons, are observed, one for the free ligand and one for the complex. Resonance difference is less pronounced among the quinoline protons, H15, H14 and H13 (Figure 7) shift by +0.21, +0.11 and -0.10 ppm, respectively, in the presence of Cd^{2+} ions. Protons H11, H10 and H9 shift by only +0.12, ca. +0.07 and +0.03 ppm, respectively. Chemical shift variation is progressively attenuated by moving along the molecular structure towards quinoline nitrogen, which allowed us to exclude its involvement in Cd^{2+} coordination.

Regardless of the resonance considered, the complete disappearance of the free ligand is observed upon the addition of 0.5 equivalents of Cd^{2+} (Figure S8). This is absolutely not compatible with the formation of a simple 1:1 [Cd**L2**]$^{2+}$ complex in solution and confirms the formation of a complex with 1:2 M$\mathbf{L}_2$ stoichiometry as also suggested by spectrophotometric and potentiometric measurements. Through molecular mechanics calculations using the MMFF94 force-field,[51] we compared the energy of different possible complexes formed with a different set of donor atoms between Cd^{2+} and **L2**. The [Cd(**L2**)$_2$]$^{2+}$ model with the lowest energy (1054 kcal mol^{-1}, Figure 8Figure S9, SI), was the one with three coordinating atoms per ligand molecule, in particular two S atoms (consecutive along the macrocycle structure), and the carbonyl C=O, within an overall distorted octahedral geometry around the metal ion.

Figure 89 shows the ^{1}H-NMR titration of **L1** with the Zn^{2+} ion. Signal assignment was obtained as mentioned above for **L2**.

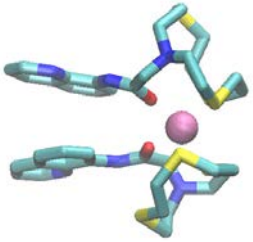

Figure S9 8. Three-dimensional model of the M$\mathbf{L}_2$ complex with the lowest energy for **L2** with Cd^{2+} ion.

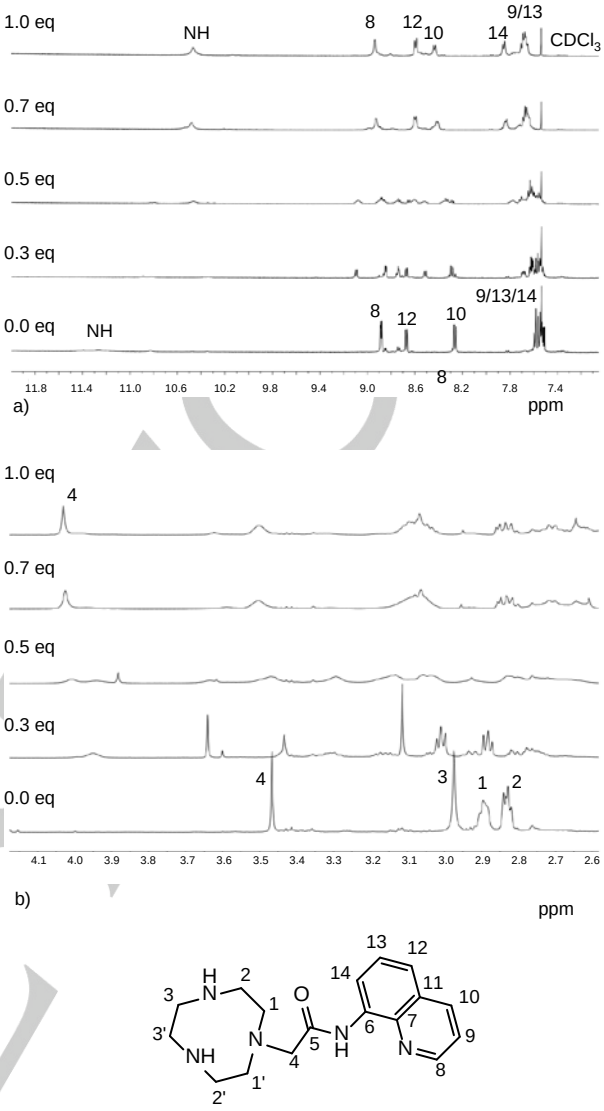

Figure 8 9. a) High and b) low field region of the ^{1}H-NMR spectra of **L1** in the presence of increasing amounts of Zn^{2+}.

Similarly to the case of **L2**, the resonance between 2.8 and 3.0 ppm, attributed to the ethylene groups of the macrocyclic unit in **L2**, changed dramatically in the presence of Zn^{2+}, especially as far as the fine structure is concerned. In particular, the proton resonance H3 changed the most, from a simple singlet to a second-order multiplet. Similar considerations as made in the case of **L2** and Cd^{2+} (see above), thus, suggest that mobility of the macrocyclic unit is lost upon Zn^{2+} coordination and confirm that the macrocyclic moiety is the main binding unit also in the case of **L1**.

Differently from **L2**, in the case of **L1** the formation of two distinct complex species during the titration are observed, the first corresponding to a 0.5:1 Zn^{2+}/**L1** molar ratio and the second to a 1:1 molar ratio, as it is evident from the inspection of all the spectral regions (Figure S10). Table 3 shows a comparison of the chemical shift variation with respect to the free ligand for the two complexes formed by **L1** with Zn^{2+}; the variations for the corresponding resonances of **L2** in the presence of Cd^{2+} ion are also shown.

Table 3. Chemical shift variations (ppm) with respect to the free ligands.

δ_{proton}[a]	$[Zn(L1)_2]^{2+}$	$[ZnL1]^{2+}$	$[Cd(L2)_2]^{2+}$
H8 (H9)	+0.22	+0.05	+0.03
H9 (H10)	n.d.	n.d.	+0.07
H10 (H11)	+0.25	+0.18	+0.12
H12 (H13)	+0.07	-0.08	-0.10
H13 (H14)	n.d.	n.d.	+0.11
H14 (H15)	+0.1	+0.26	+0.21
H4 (H5)	**+0.14**	**+0.56**	**+0.44**
H1 (H1)	n.d.	n.d.	n.d.
H2 (H2)	n.d.	n.d.	n.d.
H3 (H3/4)	n.d.	n.d.	n.d.

[a] Numbers for **L1** refers to Figure 89. Numbers in parenthesis refer to Figure 7 and pertain to **L2**. Shift variation in the resonances of methylene protons of the pendant arm are in bold.
n.d.: 'not-determined' due to spectral complexity.

It is interesting to note the similarity between the second species formed by **L1** at higher equivs. of added Zn^{2+} and the only complex $[Cd(\mathbf{L2})_2]^{2+}$ formed by **L2** with Cd^{2+}. The former species is formed at higher Zn^{2+} equivalents added and, therefore, it can be interpreted as a complex with a 1:1 Zn^{2+} to **L1** stoichiometry. The observation that the largest shift is experienced by the resonance of H4, which is the methylene group adjacent to the carbonyl, together with the overall similarity in the relative shifts for the entire molecule, suggests that, analogously to **L2**, the carbonyl group might be directly involved in the metal ion coordination. Together with the three nitrogen atoms of the macrocycle, this would lead to a complete tetrahedral coordination geometry around Zn^{2+}.
A carbonyl coordination to metal ions has been demonstrated to be possible by X-ray crystallography in the case of ligand $\mathbf{L_G}$ (Scheme 1) featuring an urea group in each pendant arm, in the complexes $[Zn\mathbf{L_G}(Ac)](Ac)$ (Ac = acetate anion) and $[Zn\mathbf{L_G}(MeCN)](ClO_4)_2$ (see SI, Figure S11). In the complex $[Cu\mathbf{L_E}](NO_3)$ ($\mathbf{L_E}$ features the same type of pendant arms as in **L1**), the complex cation $[Cu\mathbf{L_E}]^+$ features the metal center coordinated by the three nitrogen atoms of the macrocyclic moiety, the two nitrogen atoms from a deprotonated *N*-8-quinolinylacetamide group of a pendant arm, and the carbonyl oxygen atom from the acetamide group of a different pendant arm.[44]
The three-dimensional model for the 1:1 $[Zn\mathbf{L1}]^{2+}$ complex cation is shown in Figure S12 10a (see SI) and features a coordination environment around the metal centre as predicted by ^{1}H-NMR measurements. On the other hand, at lower equivalents of added Zn^{2+}, a different complex is formed during the titration with hypothesized 1:2 metal-to-ligand stoichiometry (Table 3). The intensity of the signals attributed to this species formed, reaches the maximum around 0.5 equivalents of metal ion, bolstering our hypothesis of the formation of the $[Zn(\mathbf{L1})_2]^{2+}$ species. In this case, a much lower shift variation is observed for the resonance of H4, which might suggest no involvement of the carbonyl oxygen atom in metal coordination. Molecular mechanics calculations (without the implicit presence of the solvent) indicate that the most stable $[Zn(\mathbf{L1})_2]^{2+}$ complex (220 Kcal mol^{-1}), is the one where the cation is sandwiched between the two macrocyclic unit in an octahedral geometry with heteroatoms in the pendant arms not involved in metal coordination (Figure S12 10b, SI).

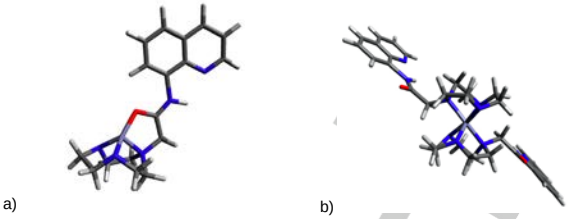

Figure S1210. **Three-dimensional model of the a) ML and b) ML_2 complex with the lowest energy for L1 with Zn^{2+}.**

Conclusion

In this paper we have further applied our synthetic approach to the development of optical selective conjugated fluorescent chemosensors. This consists in linking different fluorogenic fragments to macrocyclic receptors with unselective binding properties. [9]aneN$_3$ and [12]aneNS$_3$ macrocycles were linked to a quinoline fluorophore *via* a spacer featuring an amidic function in **L1** and **L2**, respectively. The combination of these units resulted in a selective optical response of **L1** and **L2** *via* a CHEF effect towards Zn^{2+} and Cd^{2+}, respectively, despite both ligands don't show selective binding properties towards these metal ions. In the case of **L1**, the stability of 1:1 metal-to-ligand complexes shows the following trend: $Cu^{2+}>Zn^{2+}>Hg^{2+}>Pb^{2+}>Cd^{2+}$ with an uncommonly high constant for the Zn^{2+} complex. For both **L1** and **L2**, the coordination of the carbonyl group in the pendant arm could be relevant in the synergic cooperation between the receptor and the signaling units in reaching the observed optical selectivity, which allow discrimination between Zn^{2+} and Cd^{2+} ions.

Experimental Section

Instruments and Materials. Microanalytical data were obtained using a Fisons EA CHNS-O instrument (T=1000 °C). ^{1}H- and ^{13}C-NMR spectra were recorded on a Varian VXR400 or a Varian VXR500 spectrometer, and peak positions are reported relative to tetramethylsilane ($SiMe_4$). The ^{1}H and ^{13}C-NMR spectra were carried out at 298 K using a FT-NMR Varian UNITY INOVA 500 MHz spectrometer**.** The spectrophotometric measurements were carried out at 298 K using a Thermo Nicolet Evolution 300 spectrophotometer. Uncorrected emission spectra were obtained with a Varian Cary Eclipse fluorescence spectrophotometer. Luminescence quantum yields were determined using quinine sulphate in a 1M H_2SO_4 aqueous solution (Φ=0.546) as a reference. For spectrophotometer measurements, MeCN (Uvasol, Merck) and Millipore grade water were used as solvents. Spectrofluorimetric titrations of the **L1** and **L2** with metal ions were performed by adding to a solution of the ligand (3 mL), buffered at pH 7.4 with MOPS [MOPS = 3-N-morpholino-propansulfonic acid], increasing volumes of a solution of the metal ion. Solutions of the ligands in MeCN/H_2O (1:4 v/v) were $2.24\cdot10^{-5}$- $2.58\cdot10^{-5}$ M.
Solvents for other purposes and starting materials where purchased from commercial sources where available.
2-chloro-*N*-8-quinolinylacetamide,[51] 1,4,7-triazacyclononane,[52] [1,4,7]triazacyclononane-1,4-dicarboxylic acid di-*tert*-butyl ester[53] and 1-aza-4,7,10-trithiacyclododecane[54] were prepared by published methods. Synthetic details including analytical data for **L1**-**L2** have been deposited as Supporting Information (SI).

Synthesis of *N*-8-quinolinylacetamide-1,4,7-triazacyclononane (L1).
To a solution of [1,4,7]-triazacyclononane-1,4-dicarboxylic acid di-*tert*-butyl ester (0.20 g, 0.61 mmol), K_2CO_3 (0.20 g, 1.45 mmol) and Et_3N (0.25 mL, 1.82 mmol) was added 2-chloro-*N*-8-quinolinylacetamide (0.15 g, 0.67 mmol) in anhydrous acetonitrile (20 mL). The reaction mixture was heated at 80°C for 24 hours under nitrogen. The solid was filtered off, and the solvent was removed under reduced pressure. The residue was dissolved in CH_2Cl_2 and washed with water. The organic phase was dried over Na_2SO_4, and the solvent removed under reduced pressure to give a dark yellow solid **A** (*N*-8-quinolinylacetamide-1,4,7-triazacyclononane-1,4-dicarboxylic acid di-*tert*-butyl ester,0.26 g, 85% yield). 1H-NMR ($CDCl_3$, 400 MHz): δ 1.31 (m, 18 H,CH_3), 2.79 (m, 4 H), 3.44-3.77 (m, 10 H), 7.44-7.56 (m, 3 H), 8.13-8.18 (m, 1 H), 8.77-8.89 (m, 2H), 11.10 (s, 1H, NH).
To a solution of **A** (0.26 g, 0.51 mmol) in dry CH_2Cl_2 (10 mL) was added trifluoroacetic acid (10 mL). The reaction mixture was stirred at room temperature under nitrogen for 2 hours. The solvent was removed under reduced pressure and the residue was taken in water and the pH adjusted at 10 with NaOH 10 M. The mixture was extracted three times with CH_2Cl_2 (3 x 20 mL), the organic phase was dried over Na_2SO_4 and the solvent removed under reduced pressure to give a yellow solid (0.10 g, 62% yield). ADD MP E IR
Anal. Found (Calcd) for $C_{17}H_{23}N_5O$: C, 64.8 (65.1); H, 7.1 (7.4); N, 21.8 (22.4%). ^{1}H-NMR ($CDCl_3$, 500 MHz): δ_H 2.87 (m, 4H), 2.94 (m, 4H), 3.02 (bs, 4H), 3.52 (s, 2H, NC*H*$_2$CO), 7.45 (m, 1H), 7.55 (m, 2H), 8.16 (dd, J = 8.3, 1.5 Hz, 1H), 8.74 (dd, J = 6.9, 1.9 Hz, 1H), 8.85 (dd, J = 4.2, 1.5 Hz, 1H), 11.33 (s, 1H, NH). ^{13}C-NMR ($CDCl_3$, 100 MHz): δ_C 46.9, 47.2 (N*C*H$_2$*C*H$_2$N), 63.8 (N*C*H$_2$CO), 115.6, 122.5, 122.8, 127.9, 128.7, 135.1, 136.7, 139.2, 148.5 (aromatic carbon), 171.4 (CO).

Synthesis of *N*-8-quinolinylacetamide-1-aza-4,7,10-trithiacyclododecane (L2).
To a solution of 1-aza-4,7,10-trithiacyclododecane (0.15 g, 0.67 mmol) and Et_3N (0.37 mL, 2.6 mmol) was added 2-chloro-*N*-8-quinolinylacetamide (0.22 g, 1.0 mmol) in anhydrous acetonitrile (20 mL). The reaction mixture was heated at 80°C for 48 hours under nitrogen and 24 hours at room temperature. The solid was filtered off, and the solvent was removed under reduced pressure. The residue was dissolved in CH_2Cl_2 and washed with water. The organic phase was dried over Na_2SO_4, and the solvent removed under reduced pressure to give a yellow solid (0.15 g, 55% yield).
ADD MP AND IR
Anal. Found (Calcd) for $C_{19}H_{25}N_3OS_3$: C, 55.8 (56.0); H, 5.9 (6.2); N, 9.9 (10.3); S, 23.1 (23.6%. ^{1}H-NMR ($CDCl_3$, 500 MHz): δ_H 2.86 (m, 12H), 2.99 (m, 4H), 3.43 (s, 2H, NC*H*$_2$CO), 7.46 (m, 1H), 7.55 (m, 2H), 8.17 (m, 1H), 8.77 (m, 1H), 8.86 (m, 1H), 11.19 (s, 1H, NH). ^{13}C-NMR ($CDCl_3$, 100 MHz): δ_C 31.2, 32.4 (*C*H$_2$S), 50.3 (*C*H$_2$N), 63.5 (NCH$_2$CO), 115.5, 122.3, 122.7, 127.8, 128.9, 135.2, 136.5, 138.9, 149.5 (aromatic carbon), 170.9 (CO).

Potentiometric Measurements All pH measurements (pH = −log[H$^+$]) employed for the determination of ligand protonation and metal complex stability constants were carried out in 0.10 M NaCl MeCN/H_2O (1:4 v/v) solution at 298.1 ± 0.1 K by means of conventional titration experiments under an inert atmosphere. The choice of the solvent mixture was dictated by the low solubility of the ligands and or their metal complexes in pure water. The equipment and the procedure used were previously described.[44] The standard potential $E°$ and the ionic product of water (pK_w = 14.20(1) at 298.1 ± 0.1 K in 0.10 M NaCl) were determined by Gran's method.[55] At least three measurements (with about 100 data points for each) were performed in the pH range 2–10.5. In all experiments, the ligand concentration [**L**] was about 1 × 10^{-3} M. In the complexation experiments for all systems, with the exception of the Pb^{2+}-**L1**, Hg^{2+}-**L1** and Hg^{2+}-**L2** system, in which the measurements were performed in the pH range 2-7.5, due to complex precipitation at higher pH values. Metal ion to ligand molar ratio was varied from 0.2 : 1 to 1.8 : 1. The computer program HYPERQUAD[56] was used to calculate the equilibrium constants from the emf data. In the case of Hg^{2+}, under the experimental conditions employed, the formation of metal–chloride complexes is expected to occur. The formation of such complexes was not taken into account in calculations; hence, the stability constants of Hg^{2+} complexes reported (see above) must be referred to the specific composition of the medium employed [0.10 M NaCl, MeCN/H_2O (1:4 v/v)].

Molecular mechanics. Molecular three-dimensional models were drawn with the MarvinSketch software[57] and their energy calculated in the absence of solvent through its algorithm for conformer search and geometry optimization. The MMFF94 force-field[58] was used to describe all the bonded potential energy terms. A total of 30 conformers were determined and the ones with the lowest potential energy were considered in the discussion.

Supporting Information

Supporting Information as noted in the text are provided: Synthetic details; absorption spectra of **L1** in the presence of 1 equiv. of Zn^{2+}, Hg^{2+} and Cu^{2+} (Figure S1), and **L2** in the presence of 1 equiv. of Cd^{2+}, Hg^{2+} and Cu^{2+} (Figure S2); normalized relative fluorescence emission intensity for the ion competition study of **L1** and **L2** (Figure S3); distribution diagrams of protonated species of **L1** and **L2** (Figure S4); distribution diagrams of complexes formed by **L1** and **L2** (Figures S5 and S6); distribution diagrams of complexes formed by **L2** with 0.5 equivs. of Cu^{2+}, Zn^{2+}, Pb^{2+} and Hg^{2+} (Figure S7); ^{1}H-NMR spectra of **L2** in the presence of increasing amounts of Cd^{2+} (Figure S8); Calculated 3D model with the lowest energy for the complex $[Cd(\mathbf{L2})_2)]^{2+}$ (Figure S9); ^{1}H-NMR spectra of **L1** in the presence of increasing amounts of Zn^{2+} (Figure S10); Crystallographic details for the crystal structure of $[Zn\mathbf{L_6}(MeCN)](ClO_4)_2$ (Figure S11) CCDC 2005467; 3D models with the lowest energy for the complexes $[Zn\mathbf{L1}]^{2+}$ and $[Zn(\mathbf{L1})_2]^{2+}$ (Figure S12).

Acknowledgements

We thank Fondazione di Sardegna (FdS) (Progetti biennali di Ateneo, annualità 2018) and MIUR (Ministero Italiano dell'Istruzione, Università e Ricerca, PRIN 2017 program, 2017EKCS35 project) for financial support. We thank Miss Alessandra Cabras for her contribution to the synthesis of the ligands.

Keywords: quinoline • macrocycle • fluorescent chemosensors • cadmium • zinc

[1] a) A. P. de Silva, T. S. Moodyband, G. D. Wright, *Analyst* **2009**,*134*, 2385-2393; b) D. W. Domaille, E. L. Que, C. Chang, *J. Nat. Chem. Biol*. **2008**, *4*, 168-175; b) R. Martínez-Máñez, F, Sancenón, *Chem. Rev.* **2003**, *103*, 4419-4476;
[2] a) Y. Fan, Y. F. Long, Y. F. Li, *Anal. Chim. Acta* **2009**, *653*, 207- 211; b) D.T. Quang, J.S. Kim, *Chem. Rev.* **2010**, *110*, 6280-6301.
[3] a) M. Formica, V. Fusi, L. Giorgi, M. Micheloni, *Coord. Chem. Rev.* **2012**, *256*, 170-192; b) L. Prodi, F. Bolletta, M. Montaldi, N. Zaccheroni, *Coord. Chem. Rev.* **2000**, *205*, 59-83; c) P. Pallavicini, L. Pasotti, S. Patroni, *Dalton Trans*. **2007**, 5670-5677.
[4] a) K. P. Carter, A. M. Young, A. E. Palmer, *Chem. Rev*. **2014**, *114*, 4564-4601; b) C. Lodeiro, F. Pina, *Coord. Chem. Rev*. **2009**, *253*, 1353-1383; b) H.N. Kim, W.X. Ren, J.S. Kim, J. Yoon, *Chem. Soc. Rev.* **2012**, *41*, 3210-3244; c) J.F. Zhang, Y. Zhou, J. Yoon, J.S. Kim, *Chem. Soc. Rev.* **2011**, *40*, 3416-3429;
[5] a) T. L. Mako, J. M. Racicot, M. Levine, *Chem. Rev*. **2019**, *119*, 322−477; b) J. A. Cotruvo, Jr., A. T. Aron, K. M. Ramos-Torresa, C. Chang, *J. Chem. Soc. Rev.* **2015**, *44*, 4400-4414.
[6] a) D. Wu, A.C. Sedgwick, T. Gunnlaugsson, E.U. Akkaya, J. Yoon, T.D. James, *Chem. Soc. Rev.* **2017**, *46*, 7105-7123; b)

J. Zhang, F. Cheng, J. Li, J.-J. Zhub, Y. Lu, *Nano Today* **2016**, *11*, 309-329.
[7] D. Sareen, P. Kaur, K. Singh, *Coord. Chem. Rev*. **2014**, *265*, 125-154.
[8] E. M. Nolan, S. J. Lippard, *Acc. Chem. Res*. **2009**, *42*, 193-203.
[9] Z. Dai, J. W. Canary, *New J. Chem*. **2007**, *31*, 1708-1718.
[10] a) E. L. Que, D. W. Domaille, C. J. Chang, *Chem. Rev*. **2008**, *108*, 1517-1549; b) Z. Xu, J. Yoon, D. R. Spring, *Chem. Soc. Rev*. **2010**, *39*, 1996–2006; c) K. P. Carter, A. M. Young, A. E. Palmer, *Chem. Rev*. **2014**, *114*, 4564-4601.
[11] a) A. N. Gusev, V. F. Shul'gin, S. B. Meshkova, S. S. Smola, W. Linert, *J. of Lum*. **2014**, *155*, 311–316; b) R. K. Pathak, V. K. Hinge, A. Rai, D. Panda, C. P. Rao, *Inorg. Chem*. **2012**, *51*, 4994-5005; c) M. Hagimoria, T. Utob, N. Mizuyamac, T. Temmad, Y. Yamaguchib, Y. Tominagae, H. Saji, *Sens. Actuators B* **2013**, *181*, 823-828; d) W. K. Dong, S. F. Akogun, Y. Zhang, Y. X. Sun, X. Y. Dong, *Sens. Actuat. B-Chem*. **2017**, *238*, 723-734.
[12] a) Y. Mikata, Y. Sato. S. Takeuchi, Y. Kuroda, H. Konno,S. Iwatsuki, *Dalton Trans.* **2013**, *42*, 9688-9698; b) Y. Mikata, A. Takekoshi, A. Kizu, Y. Nodomi, M. Aoyama, K. Yasuda, S. Tamotsu, H. Konno, S.C. Burdette, *RSC Adv.* **2014**, *4*, 12849-12856; c) Y. Mikata, A. Kizu, H. Konno, *Dalton Trans.* **2015**, *44*, 104-109; d) Y. Mikata, A. Takekoshi, M. Kaneda, H. Konno, K. Yasuda, M. Aoyama, S. Tamotsu, *Dalton Trans*. **2017**, *46*, 632-637.
[13] M. Taki, M. Desaki, A. Ojida, S. Iyoshi, T. Hirayama, I. Hamachi, Y. Yamamoto, *J. Am. Chem. Soc*. **2008**, *130*, 12564-12565.
[14] T. Cheng, Y. Xu, S. Zhang, W. Zhu, X. Quian, L. Duan, *J. Am. Chem. Soc*. **2008**, *130*, 16160-16161.
[15] X. Peng, J. Du, J. Fan, J. Wang, Y. Wu, J. Zhao, S. Sun, T. Xu, *J. Am. Chem. Soc*. **2007**, *129*, 1500-1501.
[16] H. N. Kim, W. X. Ren, J. S. Kim, J. Yoon, *J. Chem. Soc. Rev*. **2012**, *41*, 3210-3244.
[17] S. Ellairaja, R. Manikandan, M. T. Vijayan, S. Rajagopal, V. S. Vasantha, *RSC Adv*. **2015**, *5*, 63287-63295.
[18] a) S. Goswami, K. Aich, S. Das, C. D. Mukhopadhyay, D. Sarkar, T. K. Mondal, *Dalton Trans*. **2015**, *44*, 5763-5770; b) C. Kar, S. Samanta, S. Goswami, A. Ramesh, G. Das, *Dalton Trans*. **2015**, *44*, 4123-4132; c) K. Aich, S. Gonswami, S. Das, C. D. Mukhopadhyay, C. K. Quah, H.-K. Fun, *Inorg. Chem*. **2015**, *54*, 7309-7315.
[19] C. Kumari, D. Sain, A. Kumar, S. Debnath, P. Saha, S. Dey, *Dalton Trans*. **2017**, *46*, 2524-2531.
[20] Y. Zhang, X. Guo, M. Zheng, R. Yang, H. Yang, L. Jia, M. Yang, *Org. Biomol. Chem*. **2017**, *15*, 2211-2213.
[21] B. L. Vallee, K. H. Falchuk, *Physiol. Rev*. **1993**, *73*, 79-118.
[22] a) C. Andreini, I. Bertini, G. Cavallaro, *PLoS ONE* **2011**, 6(10): e26325; b) C. Andreini, I. Bertini, G. Cavallaro, G. L. Holliday, J. M. Thornton, *J. Biol. Inorg. Chem.* **2008**, *13*, 1205-1218.
[23] A. I. Bush, *Trends Neurosci*. **2003**, *26*, 207-214.
[24] C. J. Frederickson, J. Y. Koh, A. I. Bush, *Nat. Rev. Neurosci*. 2005, **6**, 449-462.
[25] W. Maret, Prev. Nutr. Food Sci. **2017**, *22*, 1-8.
[26] Kim, H.N.; Ren, W.X.; Kim, J.S.; Yoon, J. *Chem. Soc. Rev.* **2012**, *41*, 3210–3244.
[27] Y. Hong, S. Chen, C. W. T. Leung, J. W. Y. Lam, J. Liu, N.-W. Tseng, R. T. K. Kwok, Y. Yu, Z. Wang, B. Z. Tang, *ACS Appl. Mater. Interfaces* **2011**, *3*, 3411-3418.
[28] a) M. Saleem, K. H. Lee, *RSC Adv*. **2015**, *5*, 72150-72287; b) X. Fang, H. Li, G. Zhao, X. Fang, J. Xu, W. Yang, *Biosens. Bioelectron*. **2013**, *42*, 308-313. c) M. Hosseini, A. Ghafarloo, M.R. Ganjali, F. Faridbod, P. Norouzi, M.S. Niasari, *Sens. Actuators B* **2014**, *198*, 411-415.
[29] J. Godt, F. Scheidig, C. Grosse-Siestrup, V. Esche, P. Brandenburg, A. Reich, D. A. Groneberg, *J. Occup. Med. Toxicol*. **2006**, 1:22.
[30] M. Jaishankar, T. Tseten, N. Anbalagan, B. B. Mathew, K. N. Beeregowda, *Interdiscip. Toxicol*., **2014**, *7*, 60-72.
[31] N. Johri, G. Jacquillet, R. Unwin, *Biometals*, **2010**, *23*, 783-792.
[32] M.J.S. McLaughlin, B.R. Singh, *Cadmium in Soils and Plants*, Kliwer, Dordrecht, **1999.**
[33] S. Dobson, *Cadmium: Environmental Aspects*, World Health Organization: Geneva, **1992.**
[34] a) R. R. Lauwerys, A. M. Bernard, H. A. Reels and J.-P. Buchet, *Clin. Chem*. (Washington, D. C.), **1994**, *40*, 1391; b) S. Satarug, J. R. Baker, S. Urbenjapol, M. Haswell-Elkins, P. E. B. Reilly, D. J. Williams, M. R. Moore, *Toxicol. Lett*. **2003**, *137*, 65.83; c) M. Waisberg, P. Joseph, B. Hale, D. Beyersmann, *Toxicology* **2003**, *192*, 95.117; d) R. K. Zalups and S. Ahmad, *Toxicol. Appl. Pharmacol*. **2003**, *186*, 163-188; e) M. Viau, V. Collin-Faure, P. Richaud, J.-L. Ravanat, S. M.Candeias, *Toxicol. Appl. Pharmacol*., **2007**, *223*, 257-266; f) T. Nawrot, M. Plusquin, J. Hogervost, , H.A. Roels, H. Celis, L. Thijs, J. Vangronsveld, E. Van Hecke, J.A. Staessen, *Lancet Oncol.* **2006**, *7*, 119–126.
[35] a) A. Bencini, V. Lippolis, *Coord. Chem. Rev.*, **2012**, *256*, 149-169; b) M. Arca, A. Bencini, E. Berni, C. Caltagirone, F. A. Devillanova, F. Isaia, A. Garau, C. Giorgi, V. Lippolis, A. Perra, L. Tei, B. Valtancoli, *Inorg. Chem*. **2003**, *42*, 6929-6939.
[36] C. Bazzicalupi, A. Bencini, E. Faggi, A. Garau, V. Giorgi, V. Lippolis, A. Perra, B. Valtancoli, *Dalton Trans*. **2006**, 1409-1418.
[37] E. Arturoni, A. Bencini, C. Caltagirone, A. Danesi, A. Garau, C. Giorgi,; V. Lippolis, B. Valtancoli, *Inorg. Chem*. **2008**, *47*, 6551-6563.
[38] M. Mameli, M. C. Aragoni, M. Arca, M. Atzori, A. Bencini, C. Bazzicalupi, A. J. Blake, C. Caltagirone, F. A. Devillanova, A. Garau, M. B. Hursthouse, F. Isaia, V. Lippolis, B. Valtancoli, *Inorg. Chem*. **2009**, *48*, 9236–9249.
[39] M. A. Tetilla, M. C. Aragoni, M. Arca, C. Caltagirone, C. Bazzicalupi, A. Bencini, A. Garau, F. Isaia, A. Antonio Laguna, V. Lippolis, V. Meli, *Chem. Comm*. **2011**, *47*, 3805-3804.
[40] a) C. Bazzicalupi, A. Bencini, S. Puccioni, B. Valtancoli, P. Gratteri, A. Garau, V. Lippolis, *Chem. Comm*. **2012**, *48*, 139-141; b) A. Bencini, C. Coluccini, A. Garau, C. Giorgi, V. Lippolis, L. Messori, D. Pasini, S. Puccioni, *Chem. Comm*. **2012**, *48*, 10428-10430.
[41] M. C. Aragoni, M. Arca, A. Bencini, C. Caltagirone, A. Garau, F. Isaia, M. E. Light, V. Lippolis, C. Lodeiro, M. Mameli, R. Montis, M. C. Mostallino, A. Pintus, M. Puccioni, *Dalton Trans*. **2013**, *42*, 14516-14530.
[42] F. Bartoli, A. Bencini, A. Garau, C. Giorgi, V. Lippolis, A. Lunghi, F. Totti, B. Valtancoli, *Chem. Eur. J.* , **2016**, *22*, 14890-14901.
[43] Y. Mikata, Y. Nodomi, A. Kizu, H. Konno, *Dalton Trans*. **2014**, *43*, 1684-1690.
[44] a) A. Garau, A. Bencini, A. J. Blake, C. Caltagirone, L. Conti, F. Isaia, V. Lippolis, R. Montis, P. Mariani, M. A. Scorciapino, *Dalton Trans*. **2019**, *48*, 4949-4960; b) C. Caltagirone, A. Bencini, F. Caddeo, A. Garau, M.B. Husthouse, F. Isaia, S. Lampis, V. Lippolis, V. Meli, M. Monduzzi, M.C. Mostallino, S. Murgia, S. Puccioni, F. Lopez, P.P. Secci, Y. Taalmon, J. Schmidt, *Org. Biomol. Chem.* **2013**, 11, 7751-7759. C. Bazzicalupi, A. Bencini, A. Bianchi, A. Danesi, C. Giorgi, C. Lodeiro, F. Pina, S. Santarelli, B. Valtancoli, *Chem. Commun.* **2005**, 2630– 2632
[45] a) R. Yang, L. Zompa, *Inorg. Chem.* **1976**, *15*, 1499-1502; b) L. Zompa, H. Diaz, T. N. Margulis, *Inorg. Chim. Acta* **1995**, *232*, 131-137.
[46] S. G. Schulman, A. C. Capomacchina, *J. Am. Chem. Soc*. **1973**, *95*, 2763-2766.
[47] A. Bencini, A. Bianchi, E. Garcia-España, M. Micheloni, J. A. Ramirez, *Coord. Chem. Rev*., **1999**, *188*, 97-156.
[48] A. M. Castillo, L. Patiny and J. Wist, *J. Magn. Reson.*, **2011**, *209*, 123–130.
[49] J. Aires-de-Sousa, M. C. Hemmer and J. Gasteiger, *Anal. Chem.*, **2002**, *74*, 80–90.
[50] D. Banfi and L. Patiny, www.nmrdb.org: Resurrecting and Processing NMR Spectra On-line, www.nmrdb.org, (accessed 24 February 2020).
[51] X. Zhou, P. Li, Z. Shi, X. Tang, C. Chen, W. Liu, *Inorg. Chem*. **2012**, *51*, 9226−9231.
[52] J. E. Richman, T. J. Atkins, *J. Am. Chem. Soc*. **1974**, *96*, 2268-2270.
[53] S. Kimura, E. Bill, E. Bothe, T. Weyhermüller, K. Wieghardt, *J. Am. Chem. Soc*. **2001**, *123*, 6025-6039.

[54] M. W. Glenny, L. G.A. van de Water, J. M. Vere, A. J. Blake, C. Wilson, W. L. Driessen , J. Reedijk, M. Schröder, *Polyhedron* **2006**, *25*, 599-612.
[55] G. Gran, *Analyst* (London) **1952**, *77*, 661-671.
[56] P. Gans, A. Sabatini, A. Vacca, *Talanta* **1996**, *43*, 1739-1753.
[57] *MarvinSketch (vol. 15.7.13.0)*; ChemAxon, **2015**.
[58] T. A. Halgren, *J. Comput. Chem.* **1996**, *17* (5–6), 490–519.

Entry for the Table of Contents

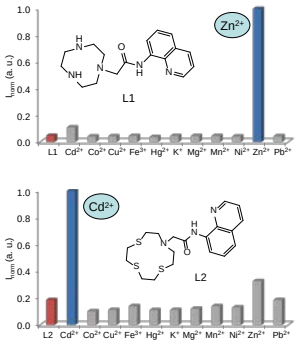

The sensing and recognition properties of two new fluorescent chemosensors featuring [9]aneN$_3$ (**L1**) and [12]aneNS$_3$ (**L2**) as receptor units and a quinoline pendant arm with an amide group as a "non-innocent" spacer, have been studied. The combination of these units resulted in a selective optical response of **L1** and **L2** *via* a CHEF effect towards Zn^{2+} and Cd^{2+}, following the formation of a 1:1 and a 1:2 metal-to-ligand complex, respectively.

Manca il 44 c